BJET
(Bayero Journal of Engineering and Technology)
https://bjet.ng/index.php/jet
Research Article
2026, Vol. 21 (3), 115-125

STRUCTURAL PERFORMANCE EVALUATION OF CONCRETE PRODUCED WITH TEPHRA AND SILICA-FUME IN PARTIAL REPLACEMENT OF CEMENT

Emmanuel Aboshio[1]; Ifeyinwa Obianyo[1] and Aboshio Aaron[2]

[1] Civil Engineering Department, Nile University of Nigeria
[2] Civil Engineering Department, Bayern University, Kano-Nigeria

Received: 23-02-2026
Revised: 03-05-2026
Accepted: 05-05-2026
Published: 27-11-2026

Abstract: *This study evaluates the mechanical and microstructural performance of Grade 40 concrete incorporating tephra and silica fume as a ternary cementitious blend. Cement was partially replaced, in equal proportions, with tephra and silica-fume at 10%, 20%, 30%, 40%, and 50% by weight. A control mix without SCMs was designed using the Department of Environment (DoE) method with a water–cement ratio of 0.40. Fresh concrete properties were assessed using the slump test, while hardened properties were evaluated through compressive strength testing of 150 × 150 × 150 mm cubes at 3, 7, 28, and 56 days, and flexural strength testing of 100 × 100 × 750 mm prisms at 28 days. Results indicated a progressive reduction in slump with increasing SCM content due to the high water demand of the blended materials. Compressive strength increased with curing age for all mixes. At 28 days, the 20% replacement mix (10% tephra + 10% silica-fume) achieved the highest compressive strength of 55.04 N/mm², exceeding the control strength of 52.47 N/mm². Higher replacement levels reduced strength due to dilution effects. Flexural strength followed a similar trend, with the 20% replacement mix achieving 5.02 N/mm², approximately 20% higher than the control. At 52 days, the same mix attained approximately 59.89 MPa in compression and 2.1% water absorption. Higher replacements generally reduced strength and increased water absorption. The 20% mix also showed a comparatively compact matrix in the micrographs, supporting its potential for reducing cement content while retaining structural performance.*

Key words: Tephra; Silica fume; Supplementary Cementitious Materials; Compressive strength; Flexural strength; Sustainability

1. Introduction

Cement manufacture contributes substantially to industrial CO_2 emissions through limestone calcination and kiln energy use (Andrew, 2018; Scrivener et al., 2018). Partial substitution of cement with suitable supplementary cementitious materials (SCMs) can reduce clinker demand while maintaining useful concrete properties. The performance of each substitution, however, depends on its composition and replacement level.

Silica-rich SCMs such as rice husk ash, volcanic ash and silica fume have been investigated in blended concretes (Mehta & Monteiro, 2014; Thomas, 2013; Aboshio et al., 2009). Recent work on natural volcanic tuff reported a strength benefit at moderate replacement but losses at higher levels (Abutaqa et al., 2024). Studies combining silica fume with rice husk ash and bagasse ash similarly show that the response of ternary systems depends on the proportions and the properties assessed (Ahmed et al., 2022; Amin et al., 2022). These findings cannot be transferred directly to the calcium-rich tephra investigated here, whose oxide composition differs appreciably from that of commonly studied siliceous volcanic materials.

Few studies report the combined response of this locally supplied tephra and silica fume in structural-grade concrete across a broad range of equal replacement proportions. This study therefore aimed to identify a suitable replacement level in Grade 40 concrete. Specifically, it examined (i) constituent materials and fresh-concrete workability; (ii) compressive and

BJET, 2026, Vol. 21(3), 115-125

flexural strengths across the selected mixes; (iii) water absorption at 52 days; and (iv) the microstructure of the control, strongest and weakest mixes.

2. Materials and Methods

2.1 Materials

2.1.1 Cement

Portland Limestone Cement conforming to BS EN 197-1:2011 made of BUA, grade 42.5 N was used as the primary binder. The cement was fresh, free from lumps, and stored in dry conditions prior to use.

2.1.2 Tephra

The tephra used in this study was locally sourced in Nigeria and processed in commercial quantities by Arctangent Engineering Ltd. The material was supplied in powdered form and in bags of 50 kg as shown in Figure 1.

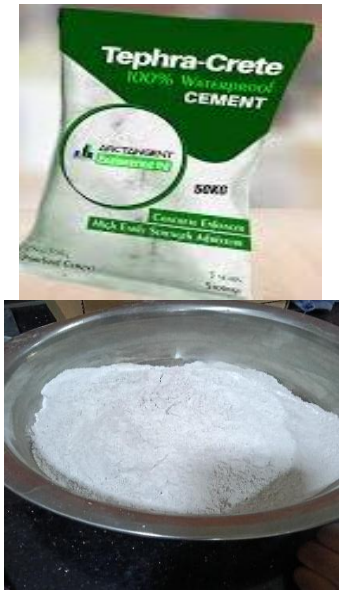


Figure 1: *Typical bag of and nature of the Tephra-crete*

2.1.3 Fine and Coarse Aggregate

Natural river sand free from organic impurities was used as fine aggregate while crushed granite with nominal maximum size, 20 mm were used in the concrete production.

2.1.4 Water

Potable water free from harmful impurities was used for mixing and curing.

2.1.5 Chemical Admixtures

A high-range water-reducing superplasticizer, Sika® ViscoCrete® Tempo 10, conforming to BS EN 934-2:2009, was used to improve workability for a low water–cement ratio of 0.40 adopted for the study.

In addition, a butadiene-based liquid polymer (styrene–butadiene rubber, SBR type) was incorporated as a polymer modifier to enhance cohesion between constituents and improve durability performance.

Both admixtures were added at 1% by weight of cement content and introduced during mixing to ensure uniform dispersion within the concrete matrix.

2.2 Methods

2.2.1 Material Characterization Tests

Material characterization tests were carried-out on the aggregates, tephra, and silica fume to determine their physical and chemical properties prior to concrete production. All applicable procedures were conducted in accordance with relevant British Standards (BS EN).

Particle size distribution of the fine and coarse aggregates was determined by sieve analysis in accordance with BS EN 933-1:2012 and the specific gravity of aggregates was determined in accordance with BS EN 1097-6:2013.

Chemical oxide composition of tephra and silica fume were determined using X-Ray Fluorescence (XRF) spectroscopy. To which the preparation and chemical analysis procedures were conducted in accordance with relevant cement chemistry testing protocols that is aligned with BS EN 196-2:2013

2.2.2 Mix Design and Proportions

The Concrete employed in this study was designed using the Department of Environment (DoE) method to achieve Grade 40 strength at 28 days with a water–cement ratio of 0.40. Mix proportion from the mix is presented in Table 1.

Table 1: *Control Mix Proportions (per m³)*

Material	Quantity (kg/m³)
Cement	450
Fine Aggregate (Sand)	665
Coarse Aggregate	1131
Water (w/c = 0.40)	180
Superplasticizer	1% of cement (4.5 kg)
SBR Polymer	1% of cement (4.5 kg)

2.2.3 Concrete Mixes

BJET, 2026, Vol. 21(3), 115-125

For the concrete production, cement was partially replaced by a combination of tephra and silica fume in equal proportions at the levels presented in Table 2. Batching of both the Tephra and Silica fume as well as all other constituents of the concrete were carried out by weight.

Table 2: *Tephra and Silica Fume Replacement of Cement in the Concrete considered in the study*

Mix ID	Total Replacement (%)	Tephra (%)	Silica Fume (%)
CTRL	0	0	0
T10SF10	20	10	10
T15SF15	30	15	15
T20SF20	40	20	20
T25SF25	50	25	25

2.2.4 Concrete Mixing Procedure

Concrete mixing was carried out using an electricity-powered tilting drum mixer of laboratory capacity to ensure uniform blending of all constituents. The mixer drum was cleaned and dampened to prevent loss of paste during mixing.

Thereafter, coarse and fine aggregates were first introduced into the mixer and dry-mixed for approximately one minute to achieve uniform distribution. Cement, Tephra, and Silica fume were later added and dry-mixed with the aggregates to ensure even dispersion of the cementitious materials within the aggregate matrix. Subsequently, about two-thirds of the mixing water was gradually added while mixing continued. The remaining water was pre-mixed with the superplasticizer (Sika® ViscoCrete® Tempo 10) and the butadiene-based liquid polymer (styrene–butadiene rubber, SBR type) before being introduced into the mixer. Mixing was continued for an additional 2–3 minutes until a homogeneous and workable concrete mix was obtained.

2.2.5 Fresh Concrete Testing and Specimen Preparation

The workability of the fresh concrete was determined using the slump test in accordance with BS EN 12350-2:2019.

For specimens preparation for compressive strength testing, sampling of the fresh concrete was carried out in accordance with BS EN 12350-1:2019 using cube moulds specimens of dimensions 150 × 150 × 150 mm. The moulds were filled in layers and compacted using a laboratory vibration table as shown in Figure 3 to ensure full consolidation and removal of entrapped air. Vibration was applied carefully to avoid segregation or excessive bleeding. After compaction, the top surface was levelled and finished with a trowel.



Figure 3: *Fresh Concrete cast in Molds and on a vibration table*

2.2.6 Compressive Strength Testing

Compressive strength testing was carried out in accordance with BS EN 12390-3:2019. The specimens were removed from the curing tank at a pre-defined testing ages of 3, 7, 28, and 56 days. Testing was conducted using an ELE-manufactured compression testing machine of 2000kN capacity at a loading rate of 1 kN/s. The cube specimens were centrally positioned between the loading platens as shown in Figure 4 to ensure uniform load distribution.

BJET, 2026, Vol. 21(3), 115-125



Figure 4: *Cubes in Concrete Crushing Machine*

2.2.7 Flexural Strength Testing

Flexural strength specimens were prepared and tested in accordance with BS EN 12390-5:2019 using prism moulds of dimensions 100 × 100 × 750 mm. The moulds were filled with fresh concrete in layers and compacted using a laboratory vibration table to ensure consolidation and elimination of entrapped air. After casting, the specimens were levelled and finished using a steel trowel to obtain a smooth surface.

Flexural strength testing was carried out using the three-point loading arrangement specified in BS EN 12390-5. The specimen was positioned on supporting rollers at the prescribed span length, and load was applied at a constant rate until failure occurred. The maximum applied load at failure was recorded, and the flexural strength (modulus of rupture) was calculated.

2.2.8 Microstructural Analysis

Microstructural evaluation of the concrete mixes was conducted using Scanning Electron Microscopy (SEM) to examine morphological characteristics and matrix development. The analysis was performed on selected specimens at 28 days, particularly the control mix and the optimum replacement mix identified from mechanical performance results.

The SEM examination was carried out under high vacuum conditions at appropriate accelerating voltage to obtain clear micrographs at the NIBBRI, Laboratory office. Abuja-Nigeria.

2.2.8 Water Absorption Testing

Water absorption of the concrete at 52 days was determined from laboratory measurements with reference to BS 1881-122:2011+A1:2020, *Testing concrete — Method for determination of water absorption* and is reported in Figure 8. Percentage absorption is calculated as $100 \times (M_s - M^d)/M^d$, where M^d and M_s are the conditioned dry and saturated masses, respectively.

3.0 Results and Discussions

3.1 Specific Gravity Results

The specific gravity values of the constituent materials used in this study are presented in Table 3. The specific gravity values obtained for gravel (2.65) and river sand (2.63) fall within the typical range of 2.60–2.70 reported for normal-weight aggregates used in structural concrete (Neville, 2011; Shetty, 2012). Similarly, the specific gravity of cement (3.15) aligns with the standard value commonly reported for Ordinary Portland Cement (OPC) (Mehta & Monteiro, 2014; Neville, 2011). This confirms that the materials used in the study meet expected density characteristics for normal concrete.

Table 3: *Specific Gravity of Materials*

Material	Specific Gravity
Gravel (Coarse Aggregate)	2.65
River Sand (Fine Aggregate)	2.63
Cement (PLC)	3.15

3.2 Oxide Composition

The oxide composition results of the Portland Limestone Cement (PLC), Tephra and Silica fume used for the study are presented in Table 4. The findings are consistent with the typical chemical characteristics of Portland-based cements reported in the literature (Neville, 2011; Mehta & Monteiro, 2014).

The tephra is predominantly composed of calcium oxide (CaO) at 86.38%, with relatively low amounts of silicon dioxide (SiO_2) (4.54%), aluminum oxide (Al_2O_3) (4.19%), and iron (III) oxide (Fe_2O_3) (0.90%) while the silica fume is largely composed of silicon dioxide ($SiO_2 \approx 80\%$), confirming strong pozzolanic reactivity. Thus, the ternary system combines a calcium source (PLC and tephra) with a highly reactive silica source (silica fume) with potential for enhanced secondary C–S–H formation and microstructural densification at optimum replacement levels.

Table 4: *Oxide Composition of the Portland Limestone Cement (PLC), Tephra and Silica-fume used in the study*

Oxide	Chemical Formula	PLC (%)	Tephra (%)	Silica Fume (%)
Calcium Oxide	CaO	68.53	86.38	0.49
Silicon Dioxide	SiO_2	15.67	4.54	80.06
Aluminum Oxide	Al_2O_3	6.11	4.19	0.65
Iron (III) Oxide	Fe_2O_3	3.82	0.90	0.09
Magnesium Oxide	MgO	1.18	2.88	0.66
Sulfur Trioxide	SO_3	3.40	—	0.32
Potassium Oxide	K_2O	0.40	0.28	0.67
Strontium Oxide	SrO	0.55	0.69	0.26
Titanium Dioxide	TiO_2	0.26	0.10	—
Barium Oxide	BaO	0.03	—	0.47
Chromium (III) Oxide	Cr_2O_3	0.02	0.02	—
Vanadium (V) Oxide	V_2O_5	0.01	—	—
Manganese (II) Oxide	MnO	0.01	0.02	0.22
Nickel (II) Oxide	NiO	0.01	0.01	—
Phosphorus Pentoxide	P_2O_5	—	—	0.03
Tin (IV) Oxide	SnO_2	—	—	0.27
Antimony (III) Oxide	Sb_2O_3	—	—	0.58
Lanthanum Oxide	La_2O_3	—	—	0.24
Zinc Oxide	ZnO	—	—	0.01
Copper (II) Oxide	CuO	—	—	0.01

3.3 Slump Test Results

Results of the slump tests which is an indication of the concrete workability is presented in Figure 5. The figure shows a steady reduction in slump (at the 1% dose of the superplasticizer and liquid polyme by weight of cement) with increasing cement replacement by the tephra–silica fume blend. The control mix recorded the highest slump (≈98 mm), while the 50% replacement mix showed the lowest value (≈55 mm). The decrease in workability is mainly attributed to the high specific surface area of silica fume and the water-absorptive nature of tephra, both of which increase water demand at a constant water–cement ratio (Aïtcin, 2000; Mehta & Monteiro, 2014).

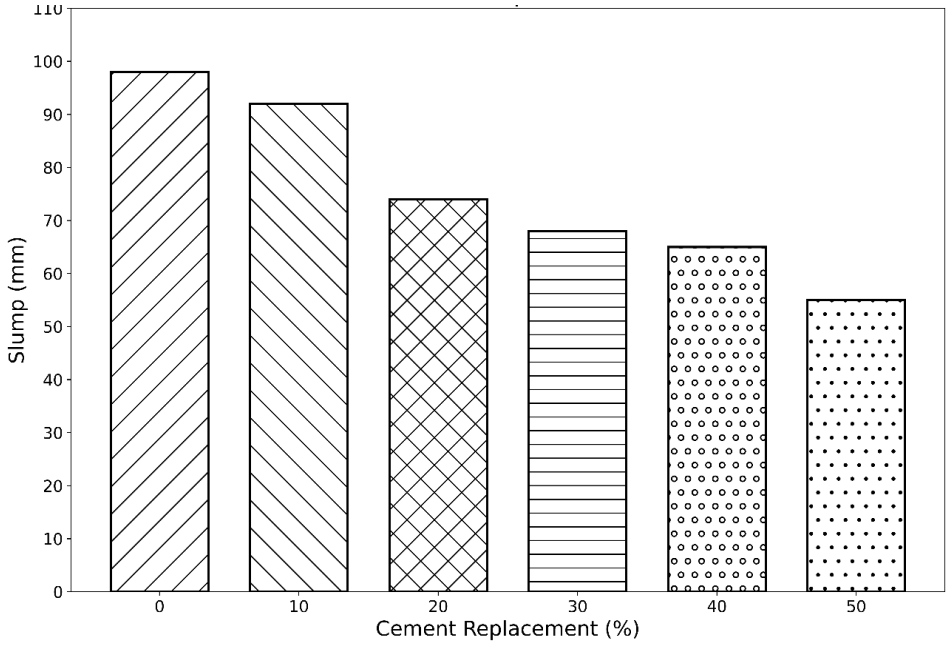


Figure 5*: Slump of concrete at the investigated cement replacement levels*

3.4 Compressive strength results

The compressive strength results presented in Figure 6 show a consistent increase in strength with curing age for all mixes, indicating continued hydration and progressive development of the cementitious matrix. The control mix achieved 52.47 N/mm² at 28 days, exceeding the target Grade 40 strength. At 10% replacement, a slight reduction in 28-day strength (50.53 N/mm²) was observed, which may be attributed to partial dilution of clinker phases. However, at 20% replacement (10% tephra + 10% silica fume), the highest compressive strength of 55.04 N/mm² was recorded, representing approximately a 5% increase over the control. Beyond this level, strength decreased progressively, with the 50% replacement mix recording 37.50 N/mm² at 28 days.

The observed strength development can be explained by the interaction of the dominant oxides within the ternary cementitious system (Amin et al., 2022). The Portland Limestone Cement (PLC), rich in calcium oxide (CaO), provides the primary source of calcium silicates (C_3S and C_2S), which hydrate to form calcium–silicate–hydrate (C–S–H), the principal strength-giving compound in concrete (Neville, 2011; Mehta & Monteiro, 2014). The tephra, also characterized by very high CaO content, contributes additional calcium to the system, enhancing calcium availability within the matrix. Meanwhile, the silica fume, containing approximately 80% silicon dioxide (SiO_2), supplies highly reactive amorphous silica. This silica reacts with calcium hydroxide liberated during cement hydration to form secondary C–S–H, resulting in matrix densification and improved strength (Aïtcin, 2000).

At 20% replacement, an optimal balance appears to exist between calcium availability and reactive silica content, promoting maximum secondary C–S–H formation without excessive reduction of clinker phases. However, at higher replacement percentages (30–50%), the dilution effect becomes dominant. The reduction in clinker content limits the formation of primary hydration products, and despite the presence of reactive silica, insufficient calcium silicates are available to sustain strength development. Consequently, compressive strength declines at higher replacement levels.

This pattern resembles the decline at high replacement in the volcanic-tuff study of Abutaqa et al. (2024),

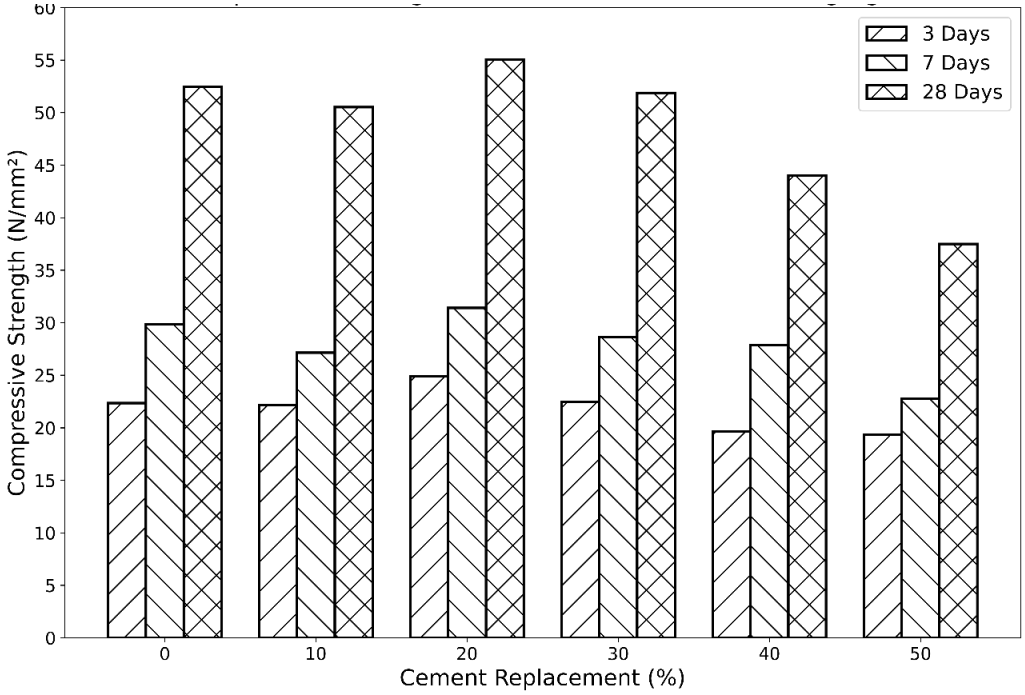


Figure 6: *Measured compressive strengths at 3, 7 and 28 days for 0–50% replacement*

3.5 Flexural Strength Test Results

The flexural strength results presented in Figure 7 show a similar trend to the compressive strength behaviour, with performance improving at moderate replacement levels and declining at higher percentages. The control mix recorded an

BJET, 2026, Vol. 21(3), 115-125

average flexural strength of 4.15 MPa at 28 days. Upon introducing the ternary blend, the strength increased to 5.02 MPa at 20% replacement, representing approximately a 21% improvement over the control. This indicates enhanced tensile resistance and improved matrix integrity at this replacement level.

At 30% replacement, the average flexural strength reduced slightly to 4.70 MPa but remained higher than the control mix. This suggests that although pozzolanic and filler effects are still beneficial, dilution of clinker content begins to influence strength development. At 40% and 50% replacement, the reduction became more pronounced (4.21 MPa and 3.87 MPa respectively). At these higher replacement levels, the reduction in primary cementitious phases (C_3S and C_2S) limits the formation of primary hydration products, and the available calcium may become insufficient to sustain optimal secondary C–S–H formation.

Other silica-fume ternary blends likewise show mix-dependent strength responses rather than a universal optimum (Amin et al., 2022).

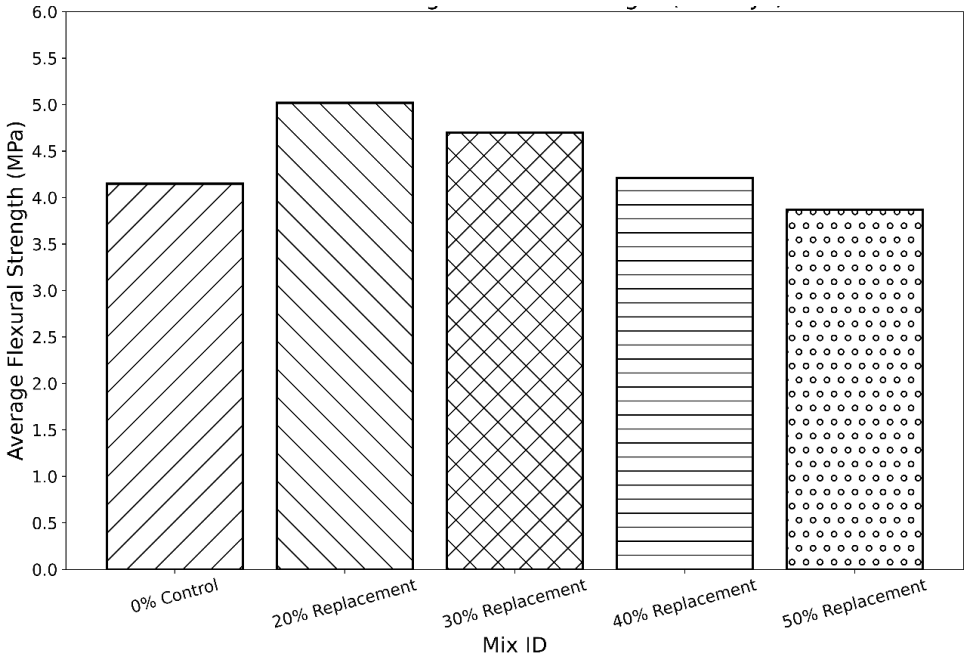


Figure 7: *Average 28-day flexural strength of the mixes*

3.6 Durability Based on Water Absorption

Water absorption is a key indicator of concrete durability as it reflects pore structure connectivity and permeability. Lower absorption values generally correspond to reduced capillary porosity, improved matrix densification, and greater resistance to aggressive agents such as chlorides, sulfates, and carbonation (Neville, 2011; Mehta & Monteiro, 2014).

Results of the water absorption tests as well as the corresponding compressive strength of the concrete at 52 days are presented in Figures 8 and 9 respectively. From the results, it can be seen that the 20% replacement mix exhibits the lowest moisture absorption (≈2.1%), compared to the control mix (≈2.4%) and higher replacement levels (up to ≈3.5% at 50%). This trend is consistent with the compressive strength development pattern and suggests that the ternary blend enhances durability at optimum replacement levels.

At higher replacement levels (40–50%), the increase in absorption indicates increased porosity. This is likely due to clinker dilution, which reduces primary hydration products (C_3S and C_2S), limiting matrix densification. Although silica fume remains reactive, insufficient calcium silicate phases may restrict optimal secondary C–S–H formation, resulting in higher pore connectivity and reduced durability potential.

Work on bagasse ash and silica-fume blends has likewise linked lower measured absorption with denser microstructures (Amin et al., 2022).

BJET, 2026, Vol. 21(3), 115-125

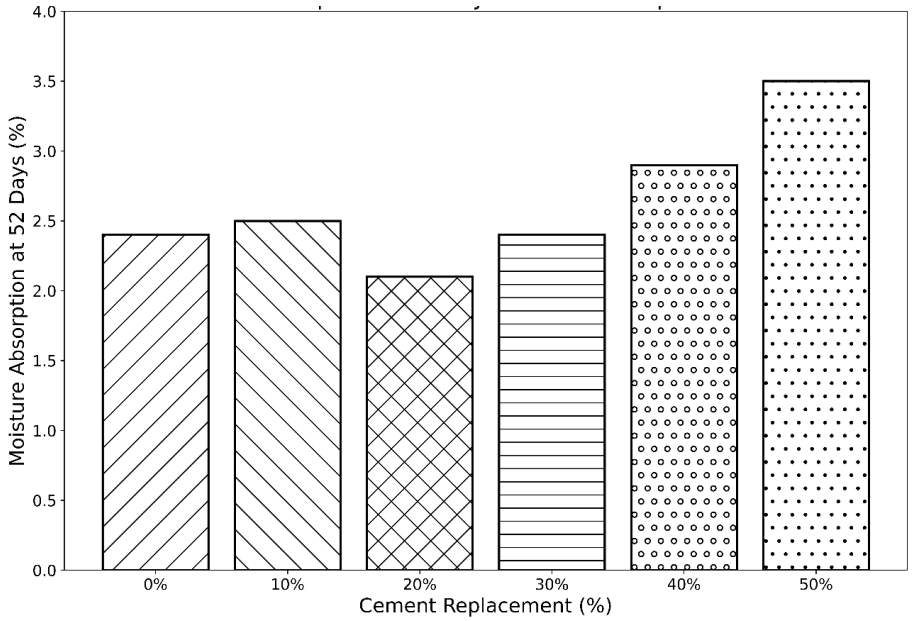


Figure 8: *Water absorption of concrete at 52 days*

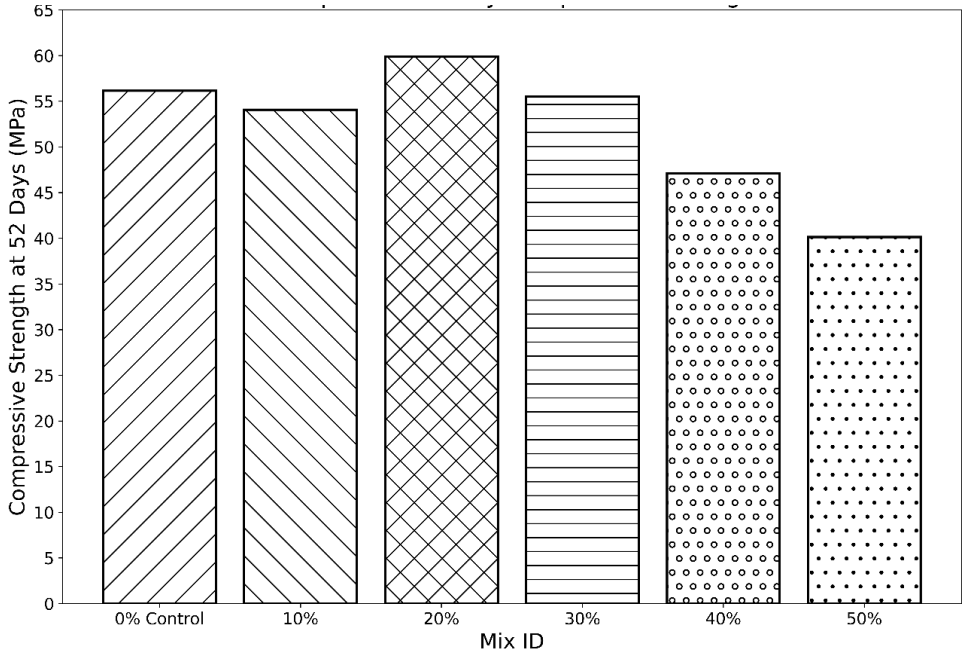


Figure 9: *Compressive Strength of the Concrete at 52 days*

4. Microstructure Characterization

4.1 Scanning Electron Microscopy (SEM) Results

The SEM micrographs of the control concrete as well as that of the optimum mix and the weakest considered based on the mechanical results i.e. mixes of 20 and 50% replacements of the cement are presented in Figures 10, 11 and 12 respectively for two magnification schemes of 50 and 10 micrometre scales.

The SEM result for the control concrete presented in Figure 10 reveal a relatively heterogeneous microstructure characterized by visible capillary voids, microcracks, and loosely packed hydration products. The matrix appears dominated by primary hydration phases, with observable plate-like calcium hydroxide (CH) crystals and fibrous calcium–silicate–hydrate (C–S–H) gel distributed within the paste.

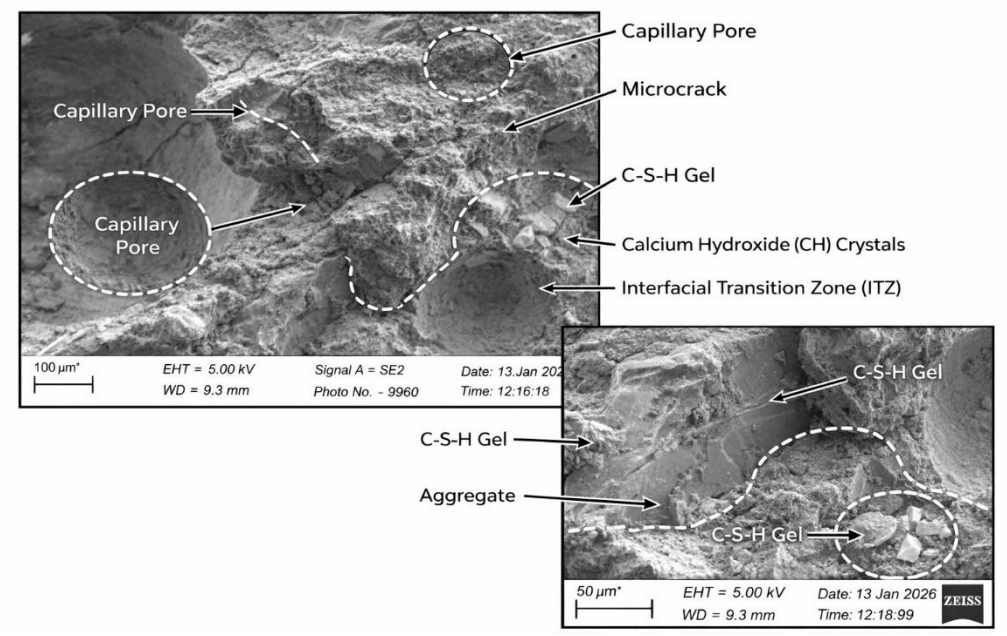


Figure 10: *SEM on 0% Replacement of cement for grade 40 concrete*

The SEM result for the 20% ternary blend presented in Figure 11 shows a markedly denser matrix with abundant secondary C–S–H gel and reduced visible porosity than that of the control mix and the 10% replacement presented in Figure 10. The interfacial transition zone appears more compact, and silica fume particles are either partially reacted or well integrated into the matrix. The synergistic interaction between CaO (from cement and tephra) and reactive SiO_2 (from silica fume) enhances secondary C–S–H formation, leading to microstructural refinement.

This densification directly correlates with the highest mechanical performance of 55.04 MPa recorded compressive strength at 28 days and 59.89 MPa at 52 days as well as 5.02 MPa flexural strength. The improvement in flexural strength particularly reflects enhanced ITZ bonding and crack resistance. Reduced pore connectivity also aligns with the lowest estimated moisture absorption, confirming improved durability.

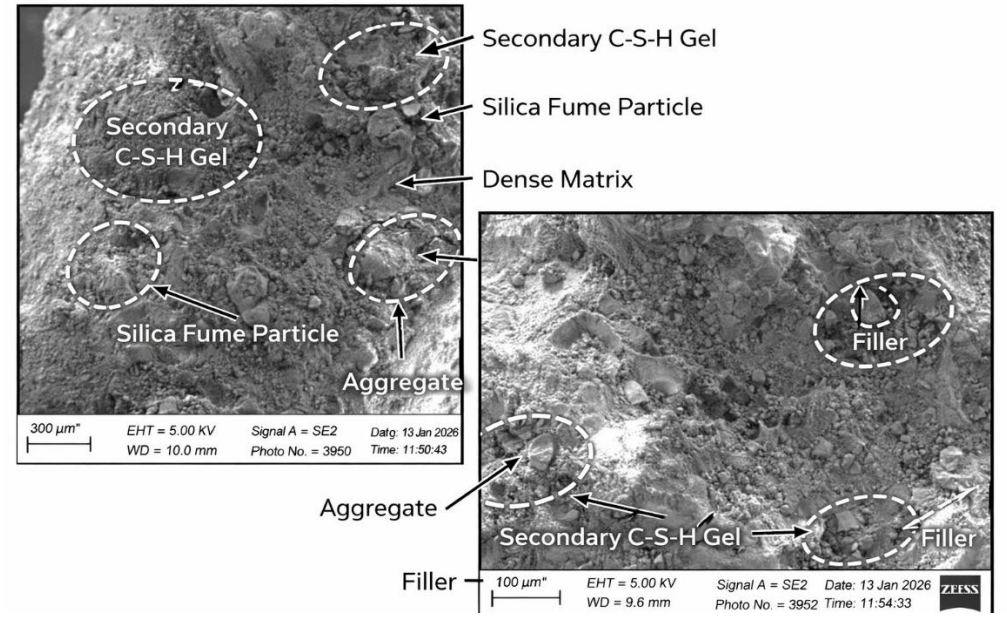


Figure 11: *SEM on 20% Replacement of cement for grade 40 concrete*

The 50% replacement microstructure presented in Figures 12 shows increased heterogeneity, with evidence of unreacted particles and localized porous regions. Although secondary C–S–H is present, clinker dilution reduces primary hydration products. The reduced availability of C_3S and C_2S limits matrix continuity and bonding strength.

This microstructural condition explains the decline in compressive strength (37.50 MPa at 28 days) and flexural strength (3.87 MPa average). Increased pore connectivity and incomplete matrix formation reduce both load-bearing capacity and tensile resistance.

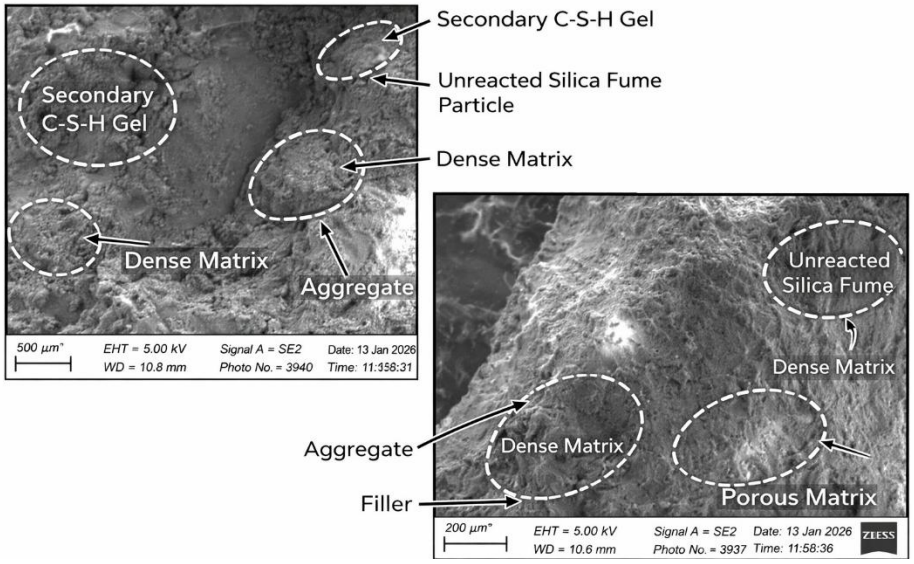


Figure 12: *SEM on 50% Replacement of cement for grade 40 concrete*

5. Conclusions

The study evaluated the structural, durability and microstructural performance of Grade 40 concrete incorporating tephra and silica fume as partial cement replacements. Based on the results, the following conclusions were drawn:

1. Portland limestone cement and tephra contained approximately 68.5% and 86.4% CaO, respectively, while silica fume contained about 80% SiO_2.
2. Concrete workability decreased with increasing replacement level. Slump reduced from 98 mm for the control mix to 55 mm at 50% replacement, but the mixes remained within workable limits.
3. The optimum replacement level was 20%, comprising 10% tephra and 10% silica fume.
4. The 20% replacement mix recorded the lowest moisture absorption, approximately 2.1% at 52 days, and offered the best resistance to moisture uptake among the mixes. Absorption increased at higher replacement levels.
5. SEM examination showed that the 20% replacement mix had a denser matrix and an improved interfacial transition zone, whereas the 50% replacement mix exhibited greater porosity.

6.0 Acknowledgement

The authors gratefully acknowledge the Tertiary Education Trust Fund (TETFund), Nigeria, for funding this research under Award No. TETF/ES/DR&D-CE/NRF2021/SETI/TRT/00080/VOL.1.

References

Aboshio, A., Ogork, E. N., & Balami, D. A. (2009). Rice husk ash as admixture in concrete. Journal of Engineering Technology, 4(2), 94–101.

Abutaqa, A., Mohsen, M. O., Aburumman, M. O., Senouci, A., Taha, R., Maherzi, W., & Qtiashat, D. (2024). Eco-sustainable cement: Natural volcanic tuffs' impact on concrete strength and durability. Buildings, 14(9), 2902. https://doi.org/10.3390/buildings14092902

Ahmed, A., Ameer, S., Abbas, S., Abbass, W., Razzaq, A., Mohamed, A. M., & Mohamed, A. (2022). Effectiveness of ternary blend

incorporating rice husk ash, silica fume, and cement in preparing ASR resilient concrete. Materials, 15(6), 2125. https://doi.org/10.3390/ma15062125

Amin, M. N., Ahmad, A., Shahzada, K., Khan, K., Jalal, F. E., & Qadir, M. G. (2022). Mechanical and microstructural performance of concrete containing high-volume of bagasse ash and silica fume. Scientific Reports, 12, 5719. https://doi.org/10.1038/s41598-022-08749-1

Aïtcin, P.-C. (2000). *High-performance concrete*. CRC Press.

Andrew, R. M. (2018). Global CO_2 emissions from cement production. *Earth System Science Data, 10*(1), 195–217. https://doi.org/10.5194/essd-10-195-2018

British Standards Institution. (2009). *BS EN 934-2:2009. Admixtures for concrete, mortar and grout – Part 2: Concrete admixtures – Definitions, requirements, conformity, marking and labelling*. BSI.

British Standards Institution. (2011). *BS EN 197-1:2011. Cement – Part 1: Composition, specifications and conformity criteria for common cements*. BSI.

British Standards Institution. (2012). *BS EN 933-1:2012. Tests for geometrical properties of aggregates – Part 1: Determination of particle size distribution – Sieving method*. BSI.

British Standards Institution. (2013). *BS EN 1097-6:2013. Tests for mechanical and physical properties of aggregates – Part 6: Determination of particle density and water absorption*. BSI.

British Standards Institution. (2013). *BS EN 196-2:2013. Methods of testing cement – Part 2: Chemical analysis of cement*. BSI.

British Standards Institution. (2019). *BS EN 12350-1:2019. Testing fresh concrete – Part 1: Sampling*. BSI.

British Standards Institution. (2019). *BS EN 12350-2:2019. Testing fresh concrete – Part 2: Slump test*. BSI.

British Standards Institution. (2019). *BS EN 12390-3:2019. Testing hardened concrete – Part 3: Compressive strength of test specimens*. BSI.

British Standards Institution. (2019). *BS EN 12390-5:2019. Testing hardened concrete – Part 5: Flexural strength of test specimens*. BSI.

British Standards Institution. (2020). *BS 1881-122:2011+A1:2020: Testing concrete — Method for determination of water absorption*. BSI

Mehta, P. K., & Monteiro, P. J. M. (2014). *Concrete: Microstructure, properties, and materials* (4th ed.). McGraw-Hill Education.

Neville, A. M. (2011). *Properties of concrete* (5th ed.). Pearson Education Limited.

Scrivener, K. L., John, V. M., & Gartner, E. M. (2018). Eco-efficient cements: Potential economically viable solutions for a low-CO_2 cement-based materials industry. *Cement and Concrete Research, 114*, 2–26. https://doi.org/10.1016/j.cemconres.2018.03.015

Shetty, M. S. (2012). *Concrete technology: Theory and practice* (7th ed.). S. Chand & Company Ltd.

Thomas, M. (2013). *Supplementary cementing materials in concrete*. CRC Press.